

Supplementary Materials

The autoimmune signature of hyperinflammatory multisystem inflammatory syndrome in children

Rebecca A. Porritt^{1,*}, Aleksandra Binek^{2,*}, Lisa Paschold^{3,*}, Magali Noval Rivas¹, Angela Mc Ardle², Lael M. Yonker^{4,5}, Galit Alter^{4,5,6}, Harsha Chandnani⁷, Merrick Lopez⁷, Alessio Fasano^{4,5}, Jennifer E. Van Eyk^{2,8,†}, Mascha Binder^{3,†} and Moshe Arditi^{1,9,†}

¹Departments of Pediatrics, Division of Infectious Diseases and Immunology, and Infectious and Immunologic Diseases Research Center (IIDRC), Department of Biomedical Sciences, Cedars- Sinai Medical Center, Los Angeles, CA, USA.

² Advanced Clinical Biosystems Research Institute, The Smidt Heart Institute, Cedars-Sinai Medical Center, Los Angeles, CA, USA.

³Department of Internal Medicine IV, Oncology/Hematology, Martin-Luther-University Halle-Wittenberg, 06120 Halle (Saale), Germany

⁴Massachusetts General Hospital, Mucosal Immunology and Biology Research Center and Department of Pediatrics, Boston, MA, USA.

⁵Harvard Medical School, Boston, MA, USA.

⁶Ragon Institute of MIT, MGH and Harvard, Cambridge, MA, USA.

⁷Department of Pediatrics, Loma Linda University Hospital, CA, USA.

⁸Barbra Streisand Women's Heart Center, Cedars-Sinai Smidt Heart Institute, Cedars-Sinai Medical Center, Los Angeles, CA, USA.

⁹Cedars-Sinai Smidt Heart Institute, Cedars-Sinai Medical Center, Los Angeles, CA, USA

* these authors contributed equally

† these senior authors contributed equally

Corresponding author:

Moshe Arditi, MD
8700 Beverly Blvd.
Davis Building, Rooms D4024, 4025, 4027
Los Angeles, CA 90048
Phone: 310-423-4471
Email: moshe.arditi@cshs.org

List of Supplementary Materials

Supplementary Materials and Methods

Supplementary Figure S1

Supplementary Figure S2

Supplementary Figure S3

Supplementary Figure S4

Supplementary Figure S5

Supplementary Figure S6

Supplementary Figure S7

Supplementary Figure S8

Supplementary Figure S9

Supplementary Figure S10

Supplementary Figure S11

Supplementary Materials and Methods

Proteomics

Depletion: On the day of depletion resin which is stored at 4 °C is equilibrated to room temperature for 30 min and mixed on a thermo mixer at 800 rpm. The resin is vortexed vigorously and 300 ul is aliquoted into the wells of a 96 well plate (Nunc™ 96-Well Polypropylene DeepWell™ Storage Plates). 10 ul of plasma is diluted 1:10 with 100 mM NH₄CO₃ and added to the appropriate wells containing depletion resin. To ensure homogenous mixing the plate is mixed at 800 rpm for 1 hr. Following this 500 ul of 100 mM NH₄CO₃ is added to each well containing samples. The diluted resin solution containing sample is aspirated and transferred to a filter plate (Nunc™ 96-Well Filter Plates). Through gentle centrifugation (100 rcf for 2 min) the low abundant protein fraction is collected into a clean 96 well plate (Beckman Coulter, deep well titer plate polypropylene). The flow through is lyophilized to dryness prior to digestion.

Digestion: Naïve and depleted serum/plasma proteins are denatured with the addition of 30 % v/v 2-2-Trifluoroethanol (TFE, Sigma) and 40 mM Dithiothreitol (DTT, Sigma) is prepared in 50 mM NH₄CO₃ (Sigma). The sample is denatured for 1 hr at 60 °C. Samples are next alkylated for 30 min at 25 °C in the dark with the addition of Iodoacetamide (Sigma, (10mM final concentration)). To prevent over-alkylation DTT is added to a final concentration of 5mM and samples are incubated for a further 15 min at 25 °C. Next, 180 ul of 50 mM NH₄CO₃ is added to dilute out TFE to a final conc of 5 %. Trypsin is added to a ratio of 25:1 and samples are incubated for 4 hr at 42 °C. Finally, the reaction is quenched with the addition of 5 ul of 25 % FA.

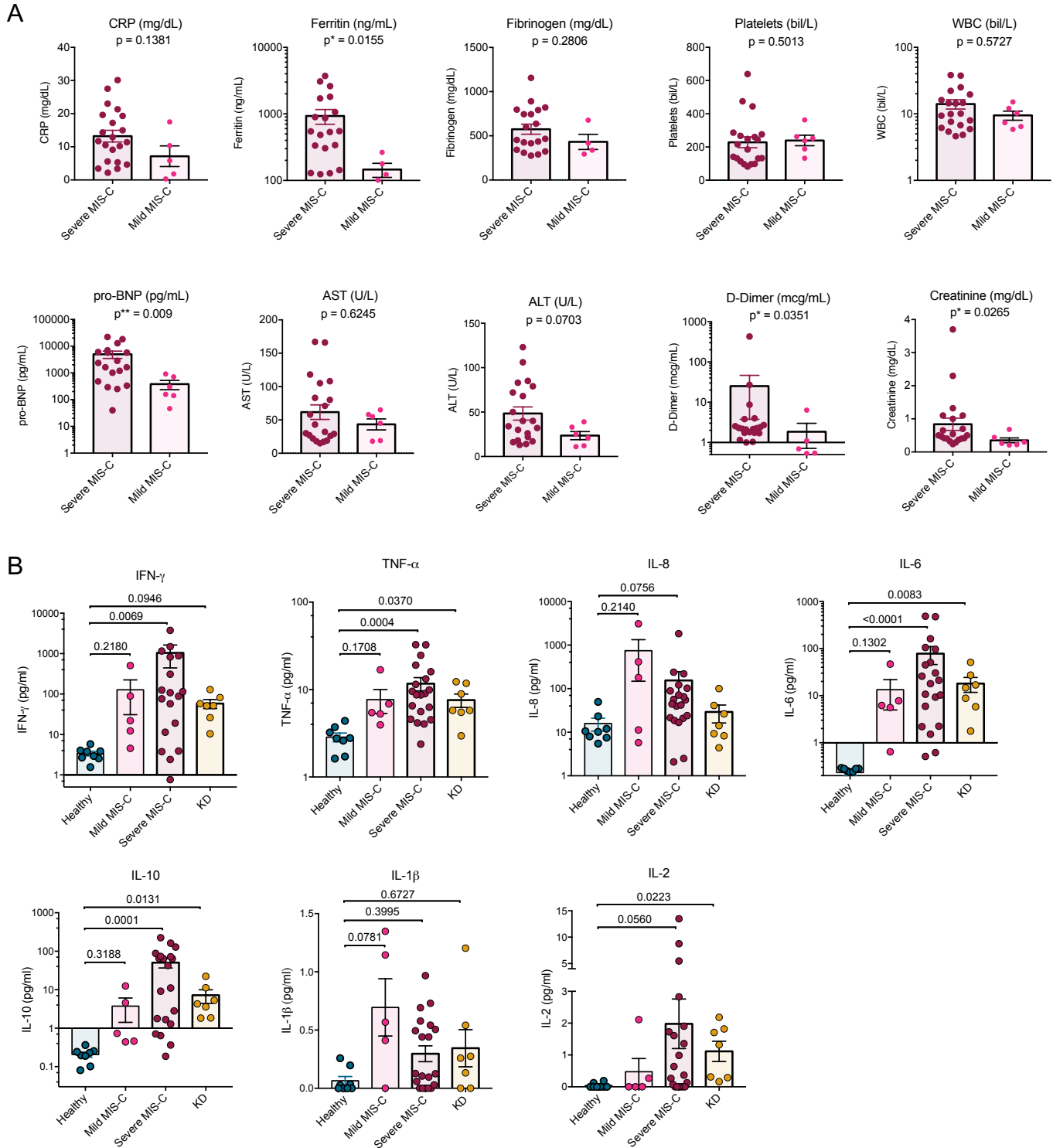
Desalting: Samples are cleaned up using Oasis 30 µm HLB 96-well Plate (Waters Co.) on the robotic workstation (Beckman i7). Digested samples (300ul) are mixed with 850 ul of 2 % phosphoric acid, 0.1% formic acid. The desalting plate is activated with addition of 1 ml of 100 % methanol. The plate is washed 3 times with the addition of 1 ml of 0.1 % formic acid. 1150 ul of the acidified sample is transferred to the plate. Then sample is cleaned with 1 ml of 0.1 % formic acid. Repeated 2 times. Then sample is eluted with 0.5 ml of 50 % acetonitrile, 0.1 % formic acid. The eluted sample is evaporated to dryness prior to resuspension in 0.1 % formic acid.

LC-MS/MS: DIA analysis is performed on an Orbitrap Exploris 480 (Thermo) instrument interfaced with a flex source coupled to an Ultimate 3000 ultra high-pressure chromatography system with mobile phase A 0.1% formic acid in water and mobile phase B 0.1 % formic acid in acetonitrile. Peptides are separated on a linear gradient of 1-27%B organic phase for 45min, 27-44% B for 15min on a C18 column (15 cm, 3 µm) over the course of total 60mins at a flow rate of 9.5 ul/min. Between every sample the column is washed with a 10 min blank where the organic phase is increased to 98 % and then re-equilibrated at 1%B for 2 minutes. Source parameters are as follows; spray voltage is maintained at 3000 kV, capillary temp is set to 300 °C and RF funnel level is set to 40. MS1 resolutions is set to 60, 000 K and AGC is set to “standard” with ion transmission of 100 ms. Mass range is set to 400- 1000 and AGC target value was for fragment spectra is set to 300 % . Peptide ions are fragmented

at a normalized collision energy of 30 %. Fragmented ions are detected across 50 DIA non-overlapping precursor windows of 12Da size. MS2 Resolution is set to 15K and ion transmission time is 25 ms. All data is acquired in profile mode using positive polarity.

Bioinformatic Data analysis: LC-MS/MS data were visually inspected using XCalibur software (4.3.73.11). DIA MS raw files were converted to mzML and the raw intensity data for peptide fragments was extracted from DIA files using the open source OpenSWATH workflow against the Human Twin population plasma peptide assay library. Retention time prediction was made using the Biognosys iRT Standards spiked into each sample. Target and decoy peptides were then extracted, scored and analyzed using the mProphet algorithm to determine scoring cut-offs consistent with 1% FDR. Peak group extraction data from each DIA file was combined using the 'feature alignment' script, which performs data alignment and modeling analysis across an experimental dataset. The total ion current (TIC) associated with the MS2 signal across the chromatogram was calculated for normalization using in-house software. This 'MS2 Signal' of each file was used to adjust the transition intensity of each peptide in a corresponding file. Normalized transition-level data was then processed using the mapDIA software to perform pairwise comparisons between groups at the peptide and protein level.

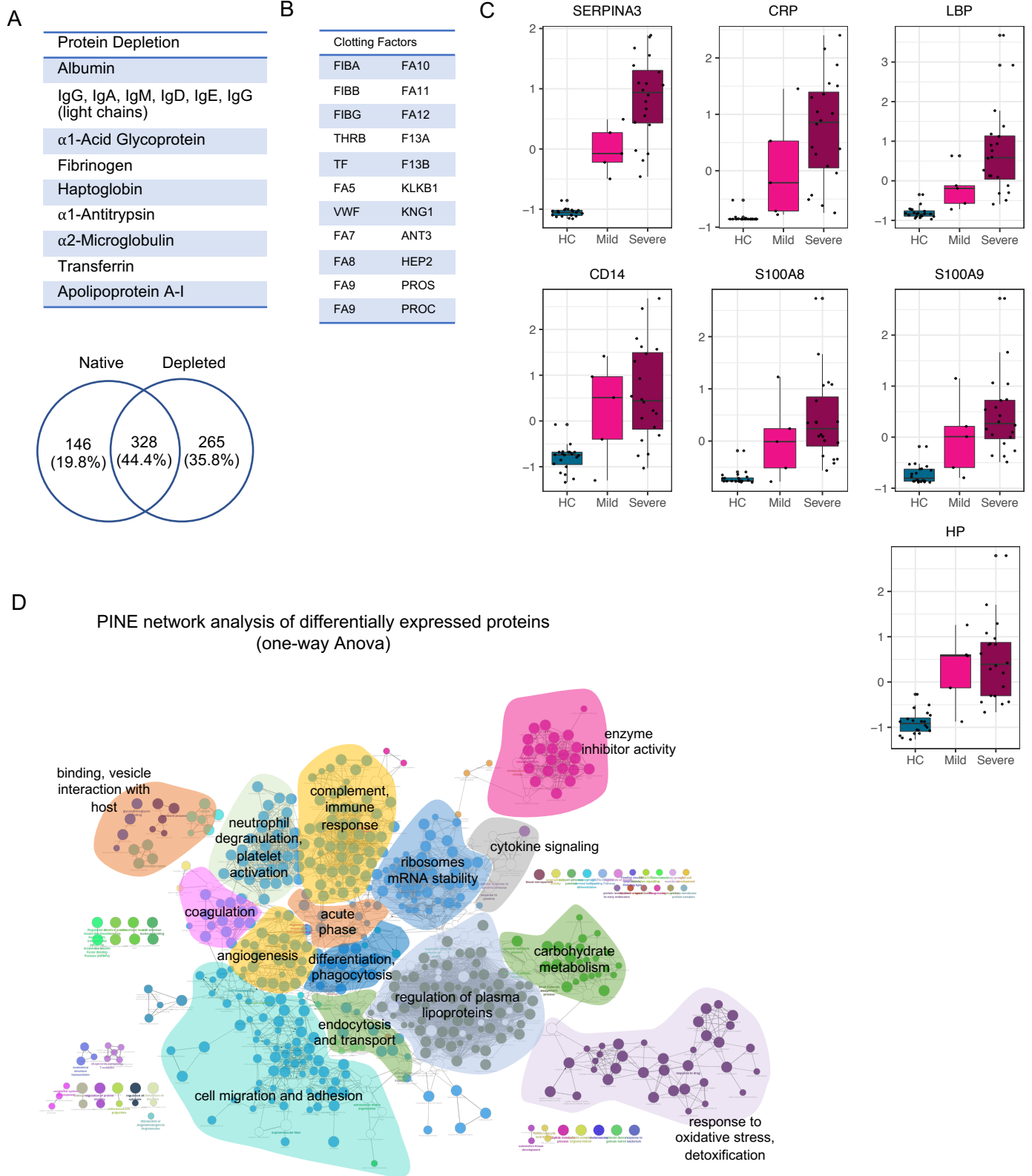
Supplementary Figure S1



Supplementary Figure S1: Clinical laboratory and cytokine profiles of mild and severe MIS-C. A. Clinical chemistry laboratory results from mild ($n = 6$) and severe ($n = 19$) MIS-C patients. Data is presented as mean \pm SEM. Statistical analysis: Mann-Whitney test. **B.** Cytokine levels in serum of healthy controls ($n = 8$), mild MIS-C ($n = 5$) and severe ($n = 20$) MIS-C patients, and in plasma of KD patients ($n = 7$). Data is presented as mean

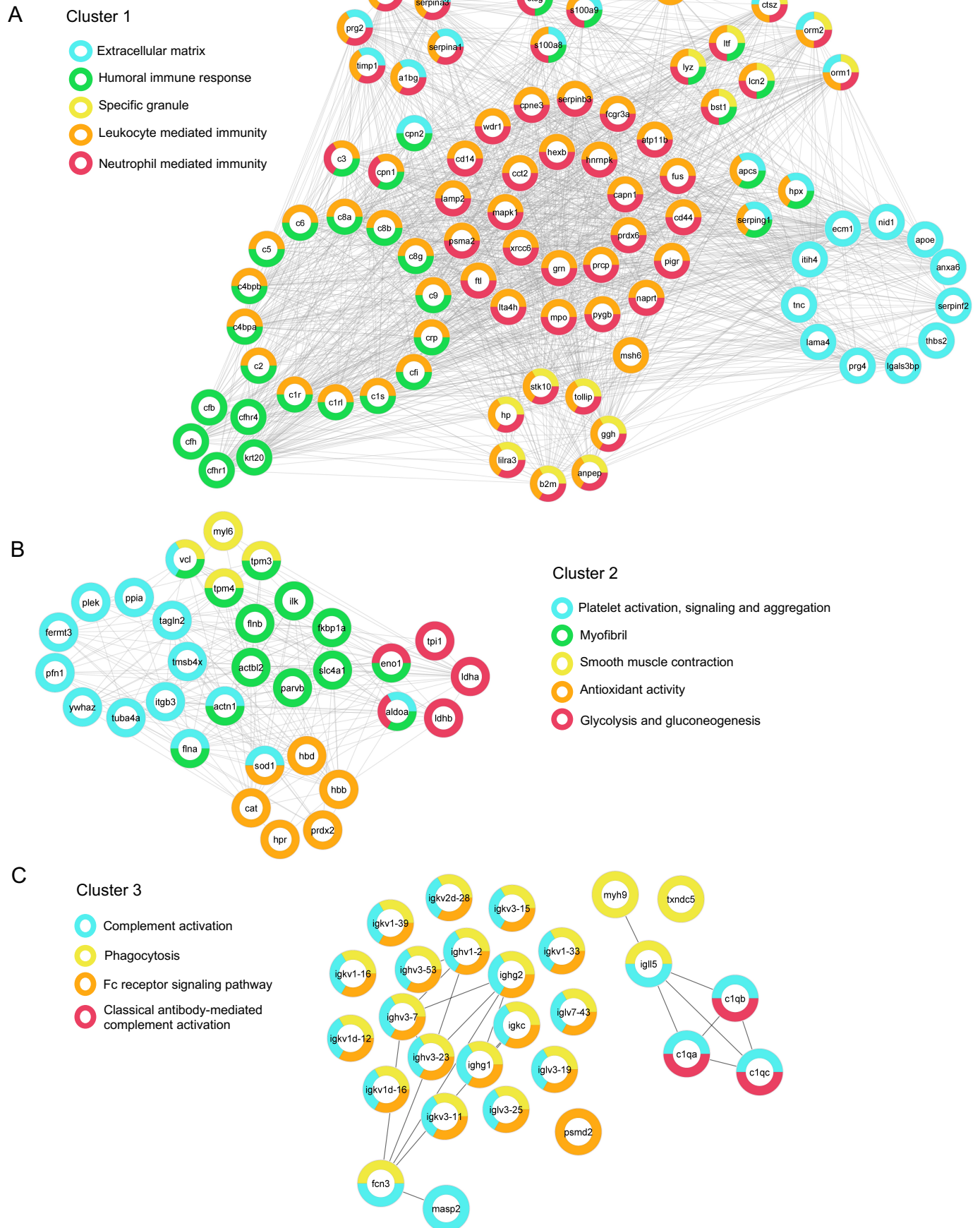
± SEM. Statistical analysis: Kruskal-Wallis one way ANOVA with Dunn's multiple comparison test. Statistical comparisons between groups not shown within graphs are not significant.

Supplementary Figure S2



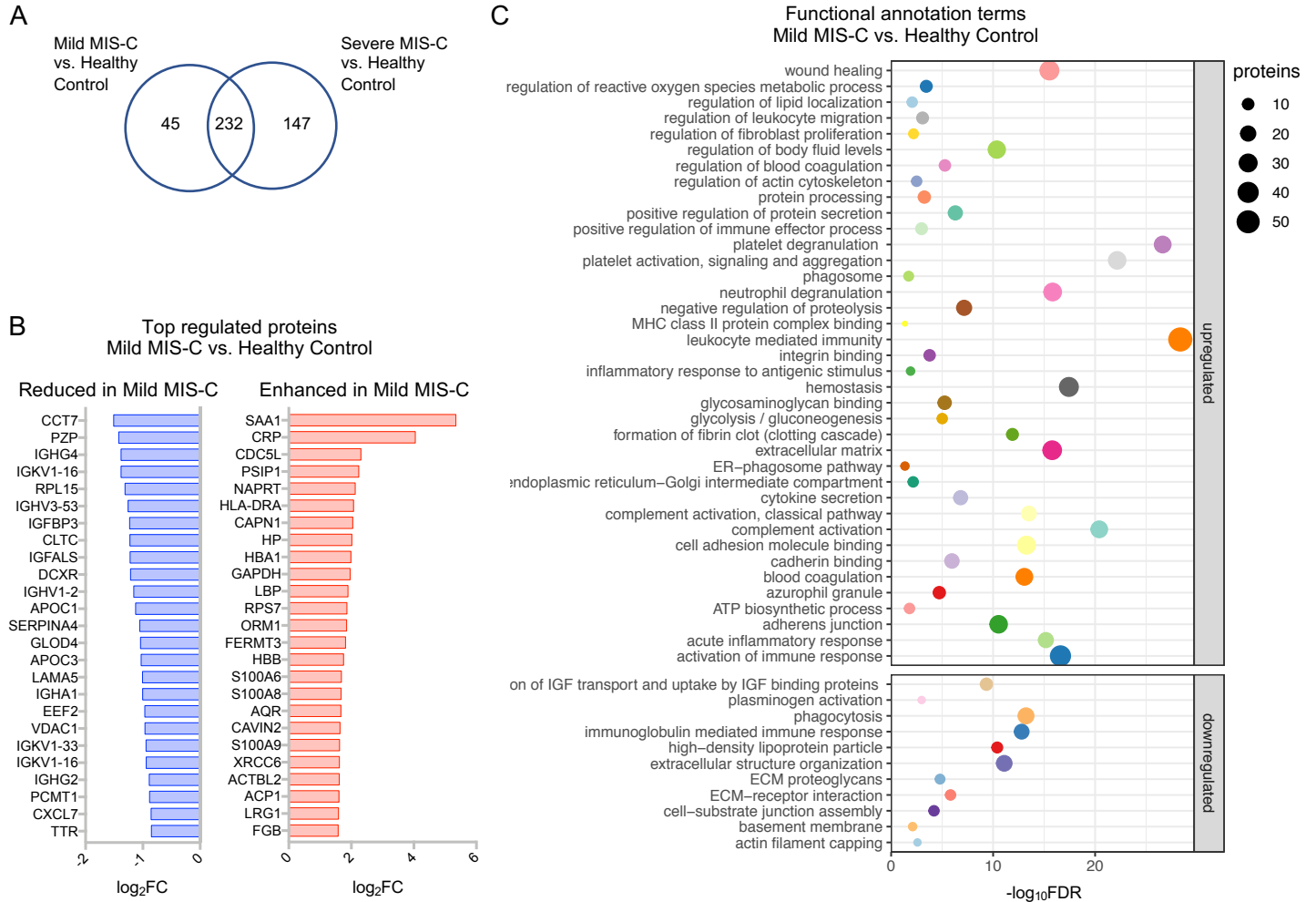
Supplementary Figure S2. A. 14 most abundant plasma proteins depleted with the High Select depletion resin (Thermo). **B.** Clotting factors removed for comparisons involving Kawasaki Disease samples. **C.** Box plots of selected proteins contributing to dimension 1 of the Principal Component Analysis presented in Figure 1B. For the improved visualization purposes boxplots are showing scaled protein expression values. Scaling was performed by mean-centering and division by standard deviation of each protein variable. **D.** Network of functionally enriched terms was generated using proteins that were found differentially regulated between sample groups (HCs', MIS-C and KD). ClueGO ontology networks are visualized using PINE software. For box plots: the bounds of the boxes represent interquartile range (IQR, Q1 to Q3) and the whiskers represent the nonoutlier minimum and maximum values $1.5 \times \text{IQR}$. The median values are marked with a horizontal line in the boxes, and outliers are marked with a black centered point outside the whisker.

Supplementary Figure S3



Supplementary Figure S3. Ontology distribution network plots of three protein expression clusters identified by Hierarchical clustering in Figure 1C. Protein nodes are colored according to the functional annotation terms which they significantly enrich.

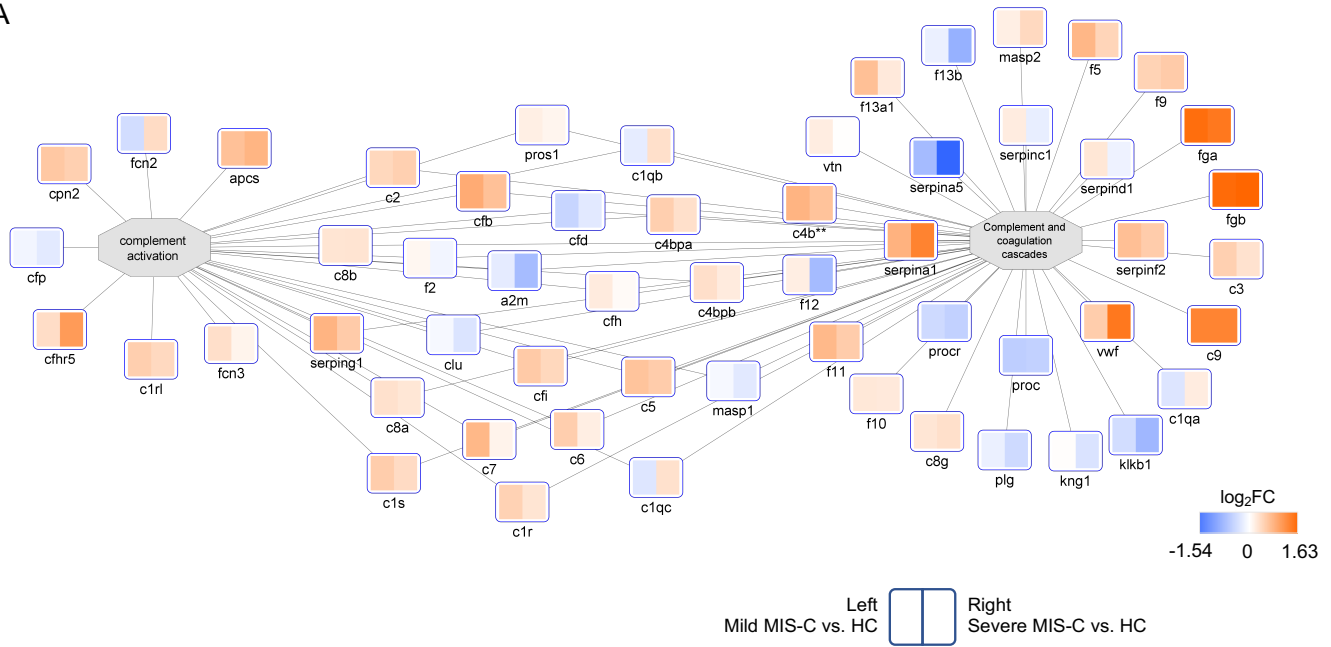
Supplementary Figure S4



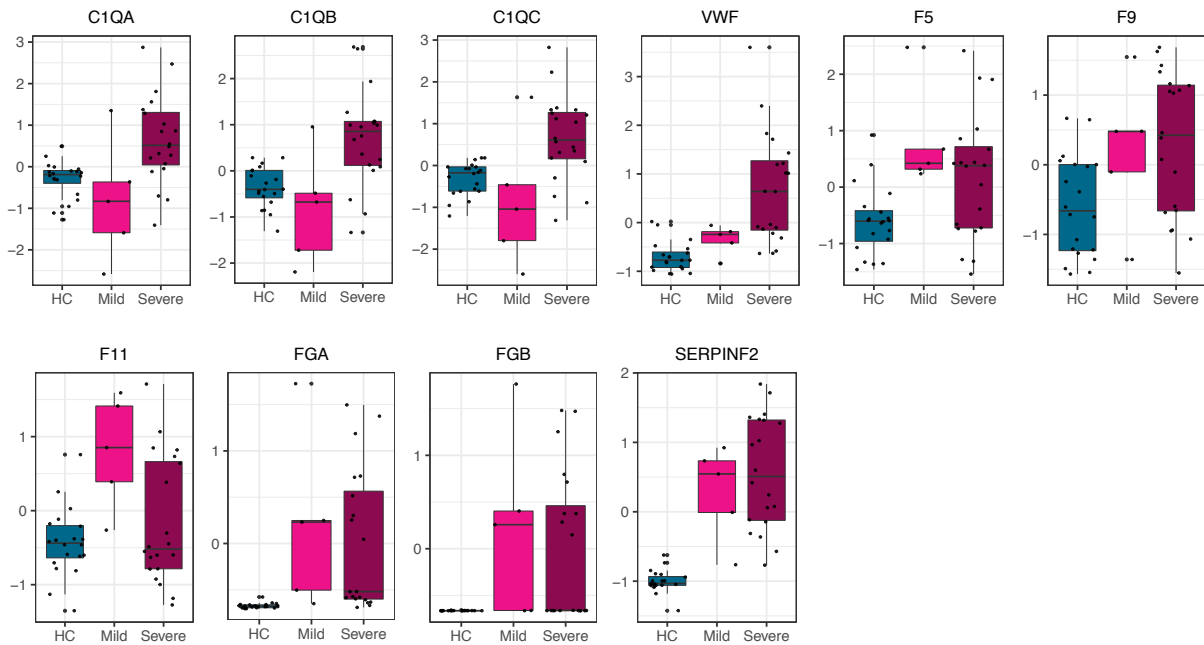
Supplementary Figure S4. A. Venn diagram of proteins found significantly regulated (FDR < 0.05) in Mild MIS-C compared with HC's or Severe MIS-C compared with HC. **B.** Top 25 proteins up and downregulated in Mild MIS-C compared with HC's. **C.** Selected functional annotation terms enriched in a set of proteins significantly up or downregulated in Mild MIS-C compared with HC's. HC = healthy controls.

Supplementary Figure S5

A



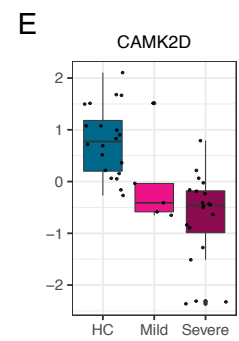
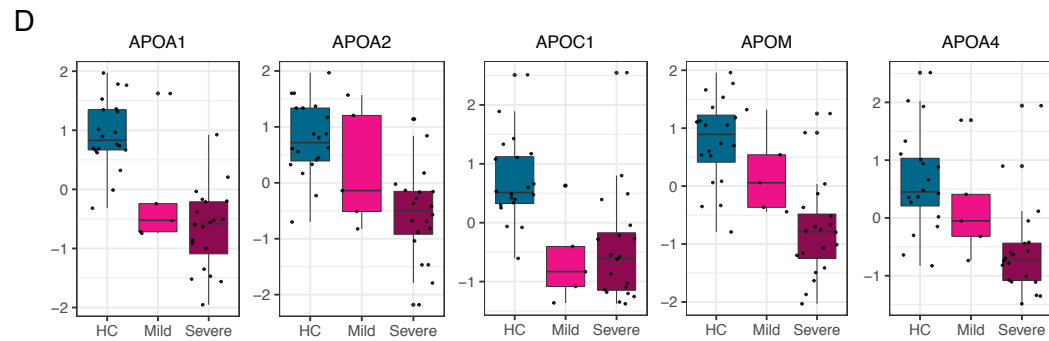
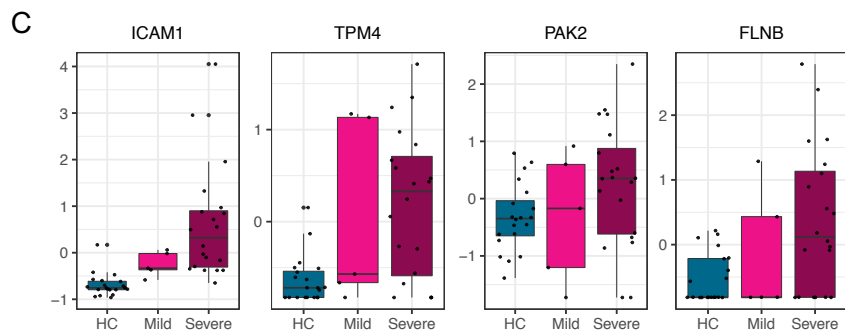
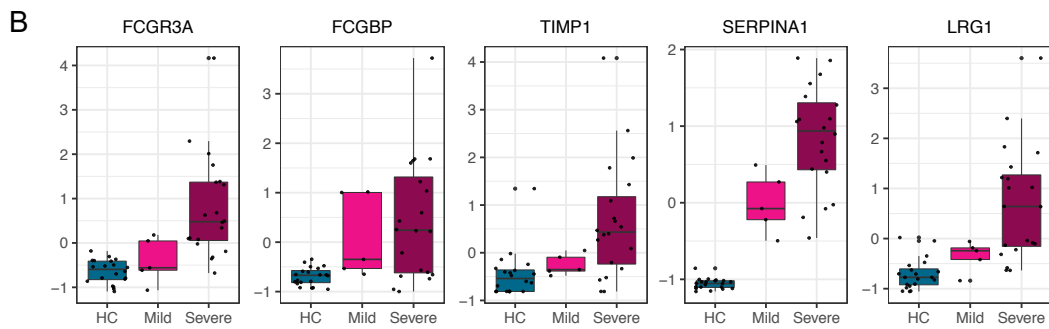
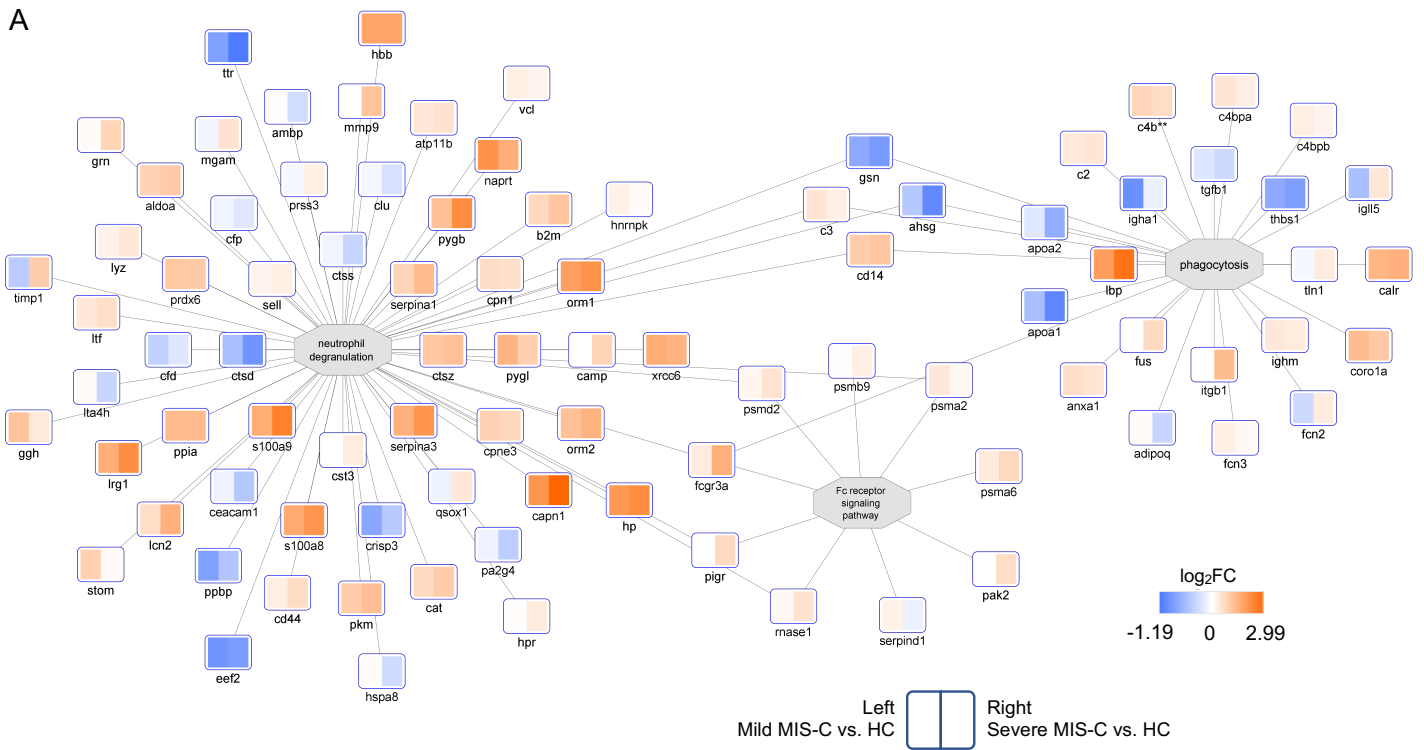
B



Supplementary Figure S5. A. Network plot showing proteins identified as significantly regulated (FDR < 0.05) in mild MIS-C (left gradient panel) or severe MIS-C (right gradient panel) compared with healthy controls from the indicated functional annotation terms. Immunoglobulin family members were excluded from the plots for clarity. Color gradient of the protein nodes is indicating natural logarithm protein fold changes (\log_2FC) between severe MIS-C or mild MIS-C vs. HC. **B.** Box plots of selected proteins from network plots depicted in panel A. For the improved visualization purposes boxplots are showing scaled protein expression values. Scaling was performed by mean-centering and division by standard deviation of each protein variable. For box plots: the bounds of the

boxes represent IQR (Q1 to Q3) and the whiskers represent the nonoutlier minimum and maximum values $1.5 \times \text{IQR}$. The median values are marked with a horizontal line in the boxes, and outliers are marked with a black centered point outside the whisker.

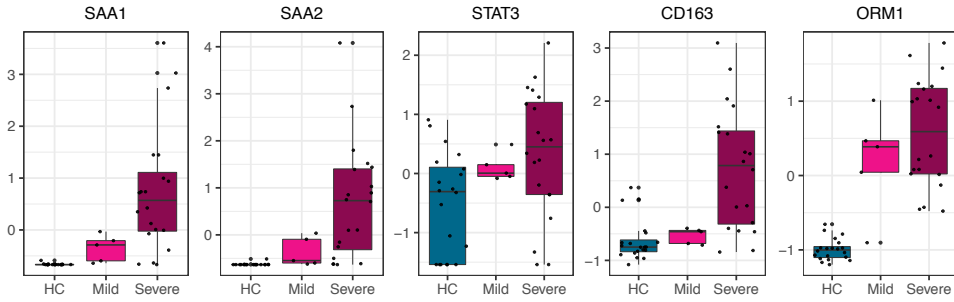
Supplementary Figure S6



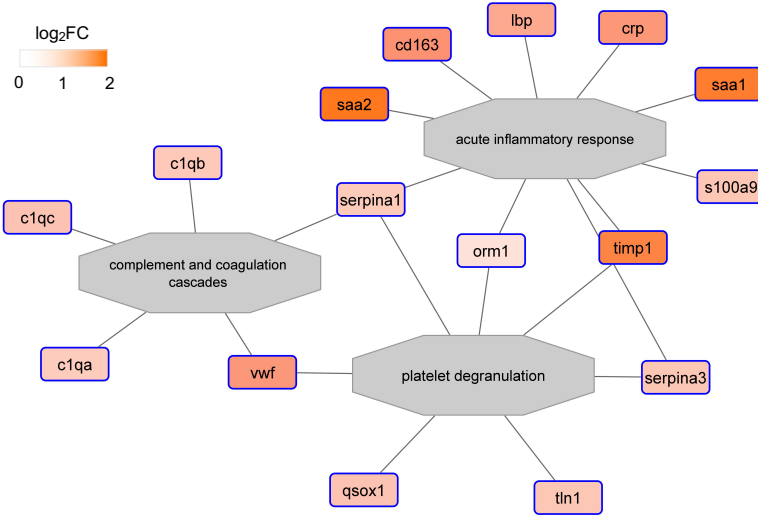
Supplementary Figure S6. A. Network plot showing proteins identified as significantly regulated (FDR < 0.05) in mild MIS-C or severe MIS-C compared with healthy controls from the indicated functional annotation terms. Color gradient of the protein nodes is indicating natural logarithm protein fold changes (\log_2FC) between severe MIS-C or mild MIS-C vs. HC. Immunoglobulin family members were excluded from the plots for clarity. **B.** Box plots of selected proteins from network plots depicted in panel A. **C.** Box plots of selected proteins involved in VEGF signaling or smooth muscle cell contraction functional annotation terms. **D.** Box plots of selected proteins involved in lipid transport, lipid metabolic processes or lipoprotein clearance functional annotation terms. **E.** Box plots of selected proteins involved in regulation of body fluids or relaxation of cardiac muscle functional annotation terms. For the improved visualization purposes boxplots are showing scaled protein expression values. Scaling was performed by mean-centering and division by standard deviation of each protein variable. For box plots: the bounds of the boxes represent IQR (Q1 to Q3) and the whiskers represent the nonoutlier minimum and maximum values $1.5 \times IQR$. The median values are marked with a horizontal line in the boxes, and outliers are marked with a black centered point outside the whisker.

Supplementary Figure S7

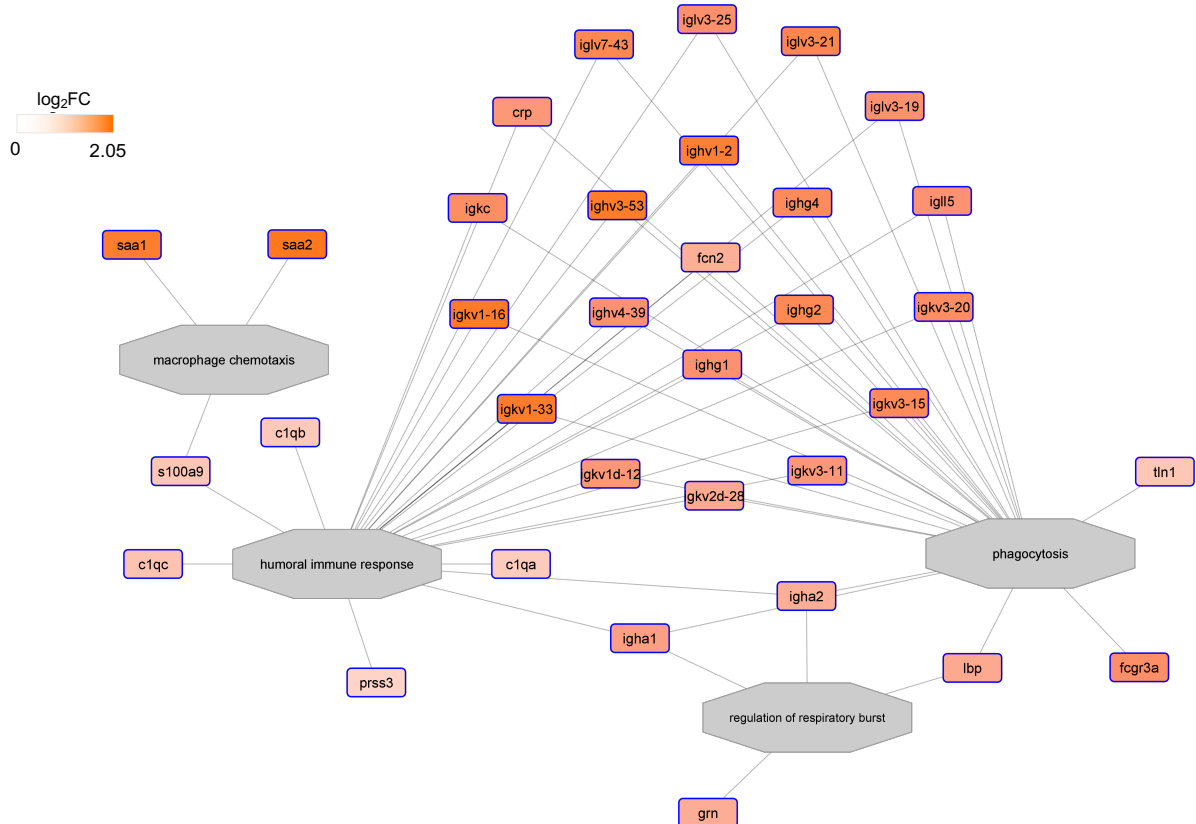
A



B

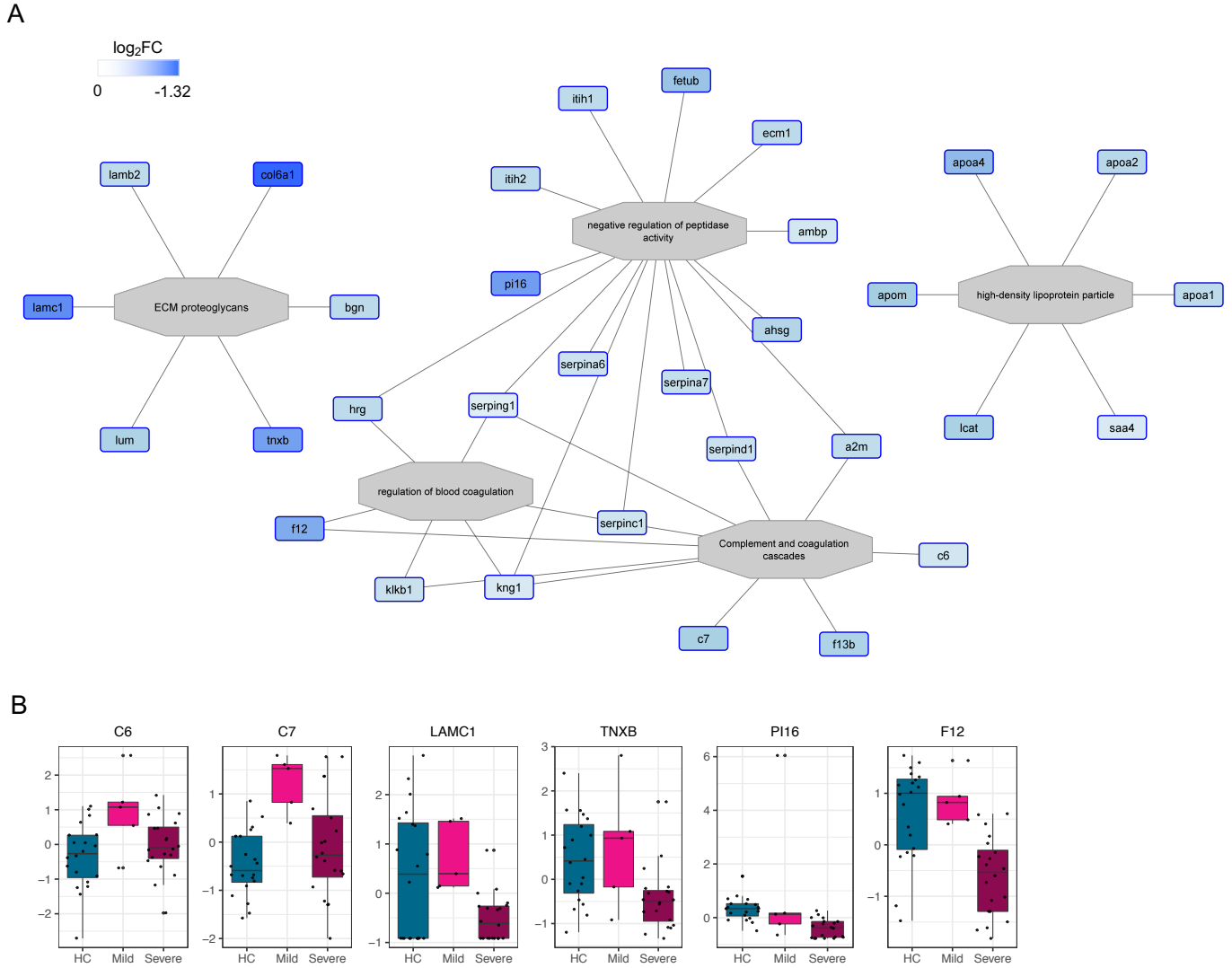


C



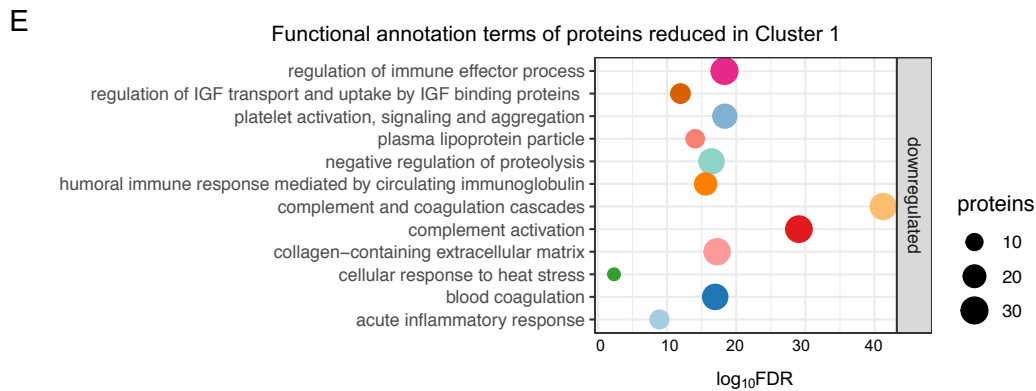
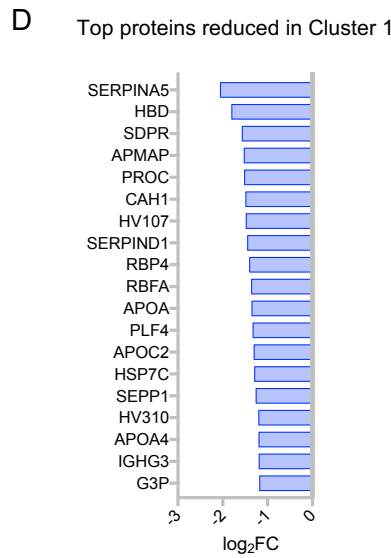
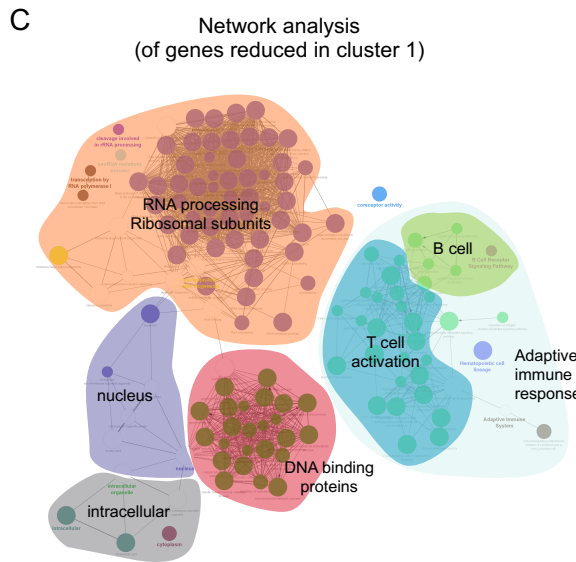
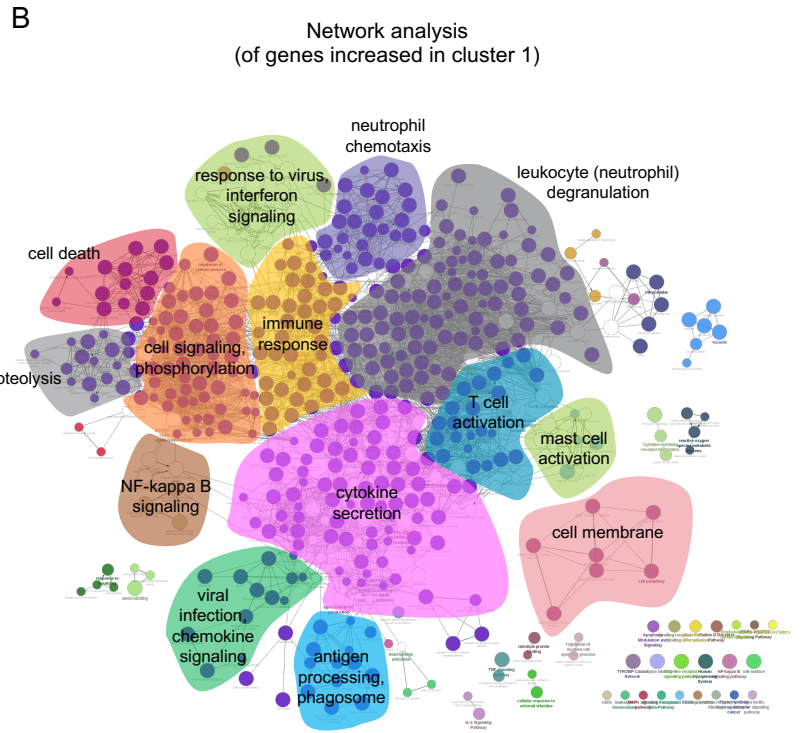
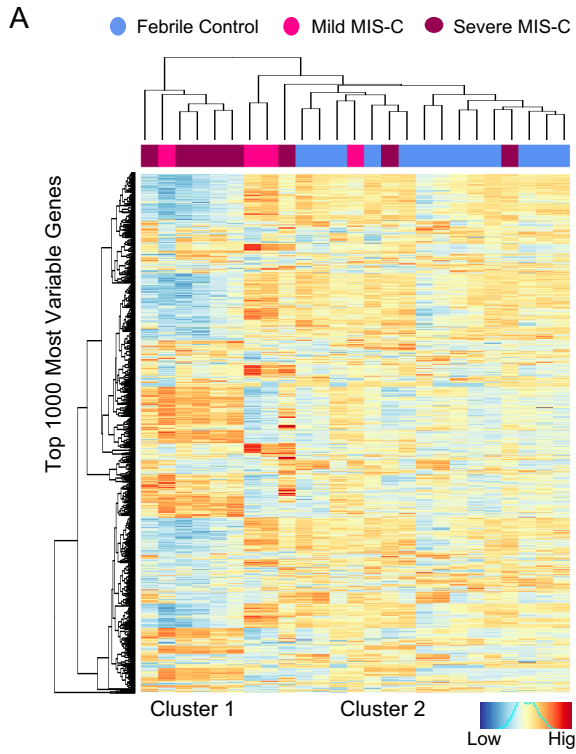
Supplementary Figure S7. A. Box plots of selected proteins found increased in severe MIS-C compared with mild MIS-C. For the improved visualization purposes boxplots are showing scaled protein expression values. Scaling was performed by mean-centering and division by standard deviation of each protein variable. **B.** Network plot shows significant proteins from selected enriched pathways. Network plot depicts annotation nodes including complement and coagulation components, acute inflammatory and platelet degranulation proteins increased in severe patients compared to mild MIS-C. Color gradient of the protein nodes indicates the natural logarithm protein fold changes (\log_2FC) between severe vs. mild MIS-C. **C.** Network plots of proteins found significantly increased in Severe MIS-C compared with Mild MIS-C in the indicated functional annotation terms. Color gradient of the protein nodes is indicating natural logarithm protein fold changes (\log_2FC) between severe MIS-C vs. mild MIS-C. For box plots: the bounds of the boxes represent IQR (Q1 to Q3) and the whiskers represent the nonoutlier minimum and maximum values $1.5 \times IQR$. The median values are marked with a horizontal line in the boxes, and outliers are marked with a black centered point outside the whisker.

Supplementary Figure S8



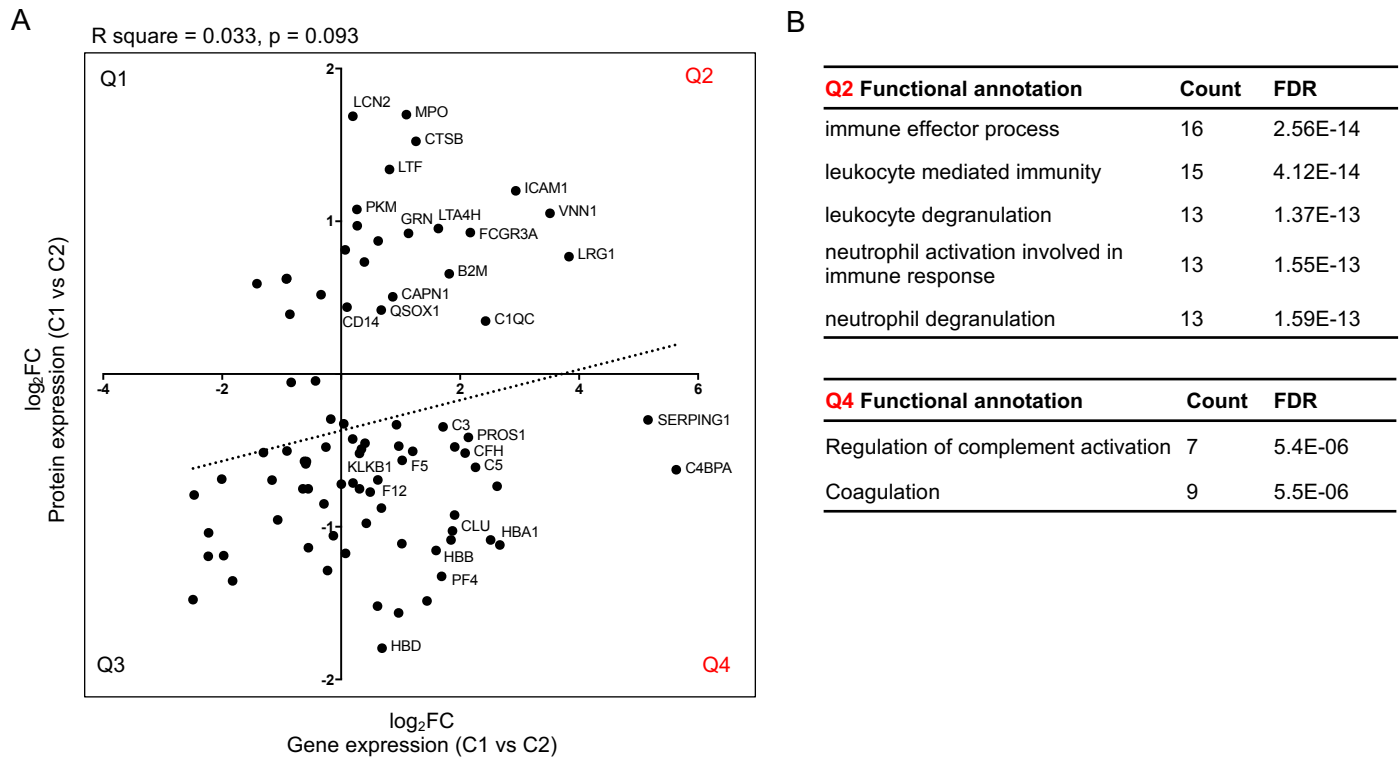
Supplementary Figure S8. A. Network plots of proteins found significantly reduced in Severe MIS-C compared with Mild MIS-C in the indicated functional annotation terms. Color gradient of the protein nodes is indicating natural logarithm protein fold changes (\log_2FC) between severe MIS-C vs. mild MIS-C. **B.** Box plots of selected proteins from panel A. For box plots: the bounds of the boxes represent IQR (Q1 to Q3) and the whiskers represent the nonoutlier minimum and maximum values $1.5 \times IQR$. The median values are marked with a horizontal line in the boxes, and outliers are marked with a black centered point outside the whisker.

Supplementary Figure S9



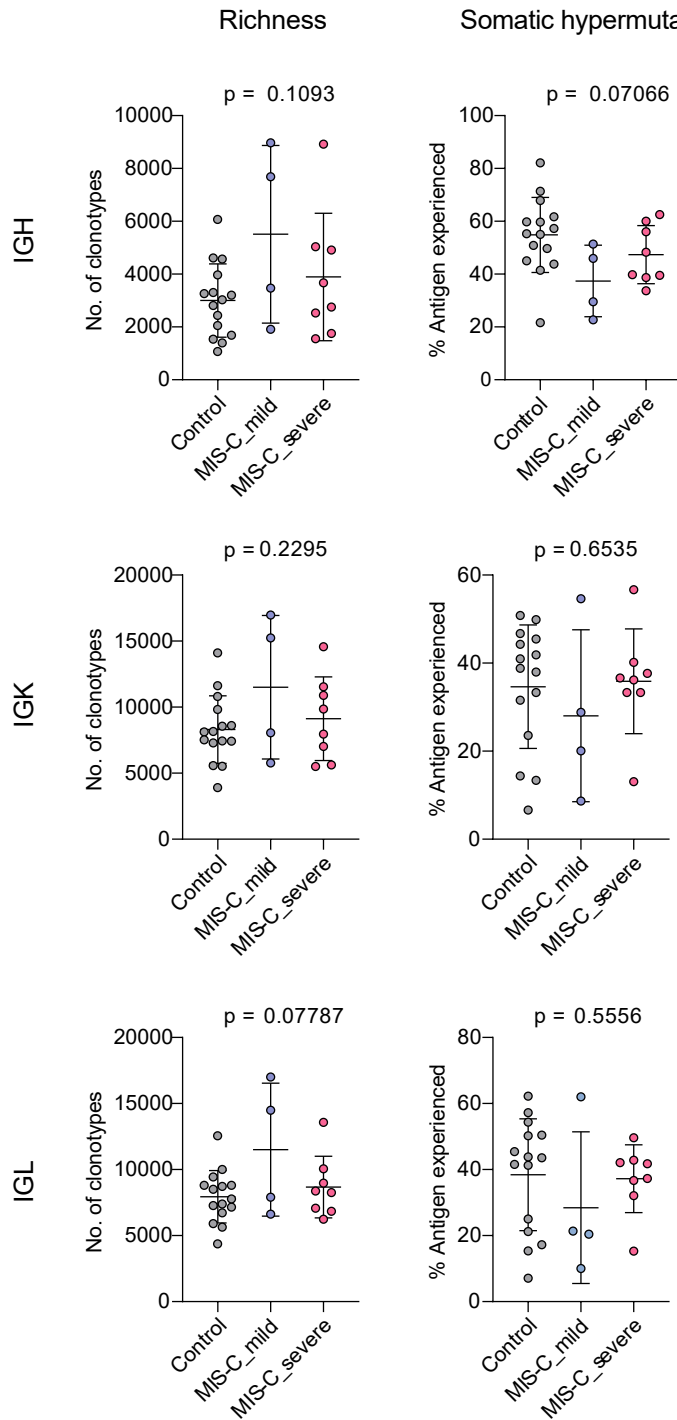
Supplementary Figure S9. A-C. RNA-seq was performed using whole blood RNA isolated from 13 febrile controls, 4 mild MIS-C and 8 severe MIS-C patients. **A.** Hierarchical clustering of top 1000 most variable genes. **B.** Network plots based on PINE analysis of genes significantly increased (FDR<0.01, log₂FC>1.5) in cluster 1 compared with cluster 2 **C.** Network plots based on PINE analysis of genes significantly reduced (FDR<0.01, log₂FC< -1.25) in cluster 1 compared with cluster 2. **D-E.** Serum proteins profiles were compared between cluster 1 and cluster 2 using available proteomics data. **D.** Top proteins reduced in cluster 1 compared with cluster 2. **E.** Selected enriched functional annotation terms and pathways based on protein expression changes significantly (FDR<0.05) downregulated in cluster 1 with respect to cluster 2.

Supplementary Figure S10



Supplementary Figure S10. A. Correlation between gene expression (log₂FC values, from RNA-seq) and protein abundance changes (log₂FC, from proteomics dataset) for comparisons between cluster 1 and cluster 2. Significant proteins are presented. Quadrant = Q. **B.** Functional annotation analysis of genes or proteins from Q2 and Q4 of correlation plot in (A).

Supplementary Figure S11



Supplementary Figure S11. B cell repertoire metrics of MIS-C patients. Richness and somatic hypermutation of productive IGH, IGK and IGL repertoires derived from the peripheral blood of mild (n=4) and severe MIS-C (n=8) patients were compared to the respective B cell repertoires derived from the blood of age-matched febrile control patients (n=15). Bars indicate mean \pm SD. Statistical analysis: Ordinary one-way ANOVA.